

Investigation of structural perfection of lithium niobate single crystals of different composition and genesis by IR spectroscopy in the area of valent vibrations of hydrogen bonds

© L.A. Bobreva¹, N.V. Sidorov¹, N.A. Teplyakova^{1,¶}, M.N. Palatnikov¹, S.A. Klimin^{2,¶¶}, N.N. Novikova²

¹Tananaev Institute of Chemistry and Technology of Rare Elements and Mineral Raw Materials, Kola Scientific Center Federal Research Center, Russian Academy of Sciences

²Institute of Spectroscopy, Russian Academy of Sciences, Troitsk, Moscow, Russia

e-mail: ¶ n.tepliakova@ksc.ru, ¶¶ klimin@isan.troitsk.ru

Received June 09, 2021

Revised September 02, 2021

Accepted September 10, 2021

We have analyzed complex defects due to the presence of hydrogen bonds in the crystal structure in nominally pure lithium niobate crystals with different Li/Nb ratio, in crystals alloyed with magnesium and zinc in a wide concentration range ($\text{LiNbO}_3:\text{Mg}$ (0.19–5.91 mol.% MgO) and $\text{LiNbO}_3:\text{Zn}$ (0.04–6.5 mol.% ZnO)) and in the double-alloyed crystals ($\text{LiNbO}_3:\text{Y}(0.24):\text{Mg}(0.63 \text{ wt.}\%)$ and $\text{LiNbO}_3:\text{Gd}(0.25):\text{Mg}(0.75 \text{ wt.}\%)$), obtained by technology of direct melt alloying, and also in the double-alloyed crystal ($\text{LiNbO}_3:\text{Mg}(5.05 \text{ mol.}\% \text{ MgO}):\text{Fe}(0.009 \text{ mol.}\% \text{ Fe}_2\text{O}_3)$) grown from a charge synthesized using the technology of homogeneous alloying with magnesium and iron Nb_2O_5 . We revealed the influence of doping impurities on the concentration of OH-groups, the type and localization of complex defects in the crystal structure. The change in the number of hydrogen atom positions in the structure of the LiNbO_3 crystal allow us to judge with sufficient accuracy whether the crystal composition is stoichiometric or congruent. For doped crystals of different compositions data were obtained testifying to changes in the character of complexation of OH-groups with point defects of the cationic sublattice with formation of defects: $\text{Me}_{\text{Li}}-\text{OH}^-$, $\text{Me}_{\text{Li}}-\text{Me}_{\text{Nb}}-\text{OH}$. A change in the mechanism of entry of the dopant cation into the structure dramatically affects the change in the properties of the crystal. The difference in the frequencies (and, correspondingly, in the values of the quasi-elastic constants of the O–H bonds) in the spectrum of a congruent crystal and doped crystals can also be contributed by differences in the electronegativity and ionic radii of the principal and doping cations.

Keywords: lithium niobate crystal, doping, complex and point structural defects, IR absorption spectroscopy, valence vibrations of OH-groups

DOI: 10.21883/EOS.2022.01.53001.12-21

Introduction

Ferroelectric single-crystal lithium niobate (LiNbO_3) features high spontaneous polarization values, high electrooptical and nonlinear optical coefficients, and a well-controlled photorefractive effect and is regarded as a versatile functional material for second-harmonic generation, electrooptical modulators, optical switches, and holographic data recording [1,2]. The possibility of adjusting the physical characteristics of crystals within a wide range by altering the state of their defect structure is a major advantage of lithium niobate. The presence of defects in the form of hydroxyl groups (OH^-) in the structure is one of the specific features of LiNbO_3 crystals grown in air [3–9]. The mechanism of inclusion of a hydrogen atom into the LiNbO_3 crystal lattice is not entirely clear. It is generally believed that this atom enters the lattice from air in the process of LiNbO_3 crystal growth [3,10]. A hydrogen atom (due to its small size) and a relatively weak hydrogen bond are highly sensitive to changes in the crystalline field induced by crystal doping and changes in the Li/Nb ratio. This results in alteration of the key parameters of the IR absorption spectrum band in

the region of valence vibrations of OH^- groups. This fact is used to study the defect structure of a crystal.

The position of hydrogen atoms bound by a hydrogen bond to an oxygen atom in the structure of nonstoichiometric crystals changes depending on the dopant type and concentration. Hydrogen atoms present in the structure of a LiNbO_3 crystal form complex defects with principal (Nb^{5+} and Li^+) and dopant (Me) cations: $V_{\text{Li}}-\text{OH}$, $\text{Nb}_{\text{Li}}-\text{OH}$, $\text{Me}-\text{OH}$, and $\text{Me}-\text{OH}-\text{Me}$ [3–9]. The presence of OH^- groups is crucial to the evolution of the secondary structure and physical characteristics of a crystal: these groups enhance the low-temperature conductivity, suppress photorefractive, and reduce the coercive field magnitude [3,7]. LiNbO_3 crystals grown in different conditions in air using different process technologies contain varying concentrations of OH^- groups. The concentration of OH^- groups may be altered by heating LiNbO_3 crystals in the corresponding atmosphere [6].

IR spectroscopy in the region of valence vibrations of OH^- groups is the technique most sensitive to the presence and localization of OH^- groups in the crystal structure. This technique allows one to study fine features of the actual

structure of LiNbO_3 crystals resulting from the specifics of localization of hydrogen atoms in the structure. This method is an express one for support of synthesis of lithium niobate crystals; it is less laborious than, e.g., Raman spectroscopy, requires less time for data accumulation in the process of spectrum measurement, and is preferable in terms of equipment maintenance costs. In addition, IR spectroscopy provides an opportunity to calculate the concentration of OH groups in the crystal structure based on the intensity of lines corresponding to valence vibrations of O–H bonds.

The aim of the present study is to determine the influence of the crystal composition on the concentration of OH^- groups and on the nature of complex defects related to OH groups in nominally pure LiNbO_3 crystals with near-stoichiometric ($\text{Li/Nb} \approx 1$) and near-congruent ($\text{LiNbO}_{3\text{cong}}$, $\text{Li/Nb} = 0.946$) compositions and in LiNbO_3 crystals with single ($\text{LiNbO}_3:\text{Mg}$ (0.19–5.91 mol.% MgO), $\text{LiNbO}_3:\text{Zn}$ (0.04–6.5 mol.% ZnO)) and double ($\text{LiNbO}_3:\text{Y}$ (0.24):Mg(0.63 wt.%), $\text{LiNbO}_3:\text{Gd}$ (0.25):Mg(0.75 wt.%), $\text{LiNbO}_3:\text{Mg}$ (5.05 mol.% MgO):Fe (0.009 mol.% Fe_2O_3)) doping synthesized using different methods.

The specific features of the structure of LiNbO_3 crystals attributable to the presence of defects in the form of hydroxyl groups (OH^-) have been examined earlier in [3–9]. However, the mechanism of fundamental rearrangement of the system of hydrogen bonds in a LiNbO_3 crystal induced by an increase in the dopant concentration still remains unclear. The studied lithium niobate crystals differ in the number and type of point defects taking the form of deep and shallow electron traps, in the degree of deformation of oxygen octahedra by the dopant (this degree defines their polarization), in the specifics of ordering of structural units of the cation sublattice along the polar axis, and, consequently, in their nonlinear optical, electrical, and photorefractive properties. Analyzing the IR spectra of actual lithium niobate crystals of different compositions and genesis, one may uncover the potential of IR spectroscopy in the region of vibrations of OH groups with regard to the estimation of structural perfection of lithium niobate crystals. This is relevant to the development of support techniques for the methods of synthesis of single crystals of lithium niobate.

Results and discussion

Positioning of a hydrogen atom in the LiNbO_3 crystal structure

Three different lengths of the O–O bond (272, 288, and 336 pm) emerge in the distorted oxygen plane of a congruent LiNbO_3 crystal, thus providing six possible positions for a hydrogen atom bound by a hydrogen bond to an oxygen atom [6]. The issue of positions of hydrogen atoms even in the structure of pure nonstoichiometric (with different Li/Nb ratios) and doped lithium niobate crystals has remained debatable for years [3–14]. The

case with doped crystals is much more complex. The localization of hydrogen atoms in the structure of doped crystals (especially in crystals with double and multiple doping that feature a complex distribution of principal and dopant cations over oxygen octahedra, which depends to a considerable extent on the concentration and type of dopant cations, and a more pronounced distortion of octahedra by dopant cations) is particularly ambiguous.

According to the data from [13], the following positions are available for hydrogen atoms in the structure of a LiNbO_3 crystal. Hydrogen may substitute directly a Li^+ ion and be located at the center of an O_6 oxygen octahedron or be positioned at the centers of O–O oxygen bonds in an octahedron occupied by a Li^+ ion (or hydrogen or a dopant ion) or in an octahedron occupied by an Nb^{5+} ion (or a dopant ion). Notably, the lengths of O–O bonds, which may accommodate hydrogen, differ significantly and depend on the composition of a crystal and on the degree of distortion of O_6 oxygen octahedra by principal and dopant cations. The nature of distribution of principal (Li^+ and Nb^{5+}) and dopant cations over octahedra and, consequently, the length of O–O bonds vary with the concentration of dopant cations in a crystal. This should result in changes in the vibrational spectrum in the region of valence vibrations of OH groups ($3500\text{--}3550\text{ cm}^{-1}$) in the IR spectrum and in the regions of vibration of oxygen ions in oxygen octahedra ($500\text{--}900\text{ cm}^{-1}$) and vibration of intra-octahedral ions ($150\text{--}300\text{ cm}^{-1}$) in the Raman spectrum.

Several models of localization of hydrogen atoms in the structure of a pure congruent lithium niobate crystal based on calculated data, NMR data, and IR absorption spectroscopy data are found in literature. The authors of [12,15] have investigated experimentally the shape of NMR lines in a congruent lithium niobate polycrystal and calculated the second moment of the NMR line of the ^1H isotope. It was concluded in these studies that a hydrogen atom should be located within a vacant $V_{\text{Li}}\text{O}_6$ octahedron at the center of the longest O–O bond (336 pm). That said, the results of computer calculations of the potential relief within the unit cell of a stoichiometric lithium niobate crystal based on the classical electrostatic approach with the modified point multipole method in [13,16] suggest that all tentative positions of hydrogen atoms at the center of O–O bonds are unstable both in the perfect structure and in the vicinity of a V_{Li} defect. At the same time, IR absorption spectroscopy data analyzed in [4] suggested that hydrogen atoms in a pure congruent crystal are located in the plane of oxygen atoms at the shortest O–O bonds (272 pm). It was assumed that the longest O–O bond (336 pm) is not occupied by hydrogen. However, this conclusion is likely to be unreliable, since the authors assumed in their calculations that a lithium niobate crystal has the perovskite structure with oxygen octahedra sharing their vertices. In fact, a lithium niobate crystal has a much more rigid pseudo-ilmenite structure with the hexagonal closest packing where oxygen octahedra share their edges [17–19]. According to the data from [20,21] obtained by analyzing

the IR absorption spectra, a hydrogen atom is likely to be positioned in the upper oxygen triangle of an NbO_6 octahedron. The dipole moment of an OH^- group is directed along the short O–O bond, and the O–H bond length is 98.8 pm [20]. The authors of [4] considered a model where four different positions of a hydrogen atom in the structure of a lithium niobate crystal are analyzed. Hydrogen in this model is located at two short O–O bonds perpendicular to the Z axis. The positioning of hydrogen along the long O–O bond (336 pm) is excluded due to the fact that the distance between a hydrogen atom and an oxygen ion (more than 99 pm) is not sufficient to form a hydrogen bond (with only the electrostatic interaction being feasible). In addition, such a weak bond is affected by the charge distribution and the ionic polarizability of the nearest ions. This influence contributes to its further weakening. Five energetically different positions of hydrogen atoms in a crystal are considered in the model described in [4]. However, unaccounted interactions of hydrogen with other ions (apart from the formation of a hydroxyl group) are considered in this model. The emergence of two high-energy bands may be attributed to intrinsic defects arising in Li-deficient crystals.

The results of computer simulation of the hydrogen atom positioning in the Born–Oppenheimer approximation in [22], which was aimed at determining the position of the most stable configuration of a defect cluster with an OH^- group in the LiNbO_3 crystal structure, revealed that hydrogen in the most stable configuration is not located at or near an O–O bond; instead, it is located near the bisecting line (3.36 Å) of an oxygen triangle and tilted by 4.3° away from the oxygen plane toward a V_{Li} lithium vacancy. The corresponding equilibrium OH bond length is 0.988 Å. These results agree with the earlier theoretical data from [23] and the results of IR spectroscopy in polarized light [24]. The position of hydrogen atoms bound by a hydrogen bond to an oxygen atom in the structure of nonstoichiometric crystals changes with the Li/Nb ratio and the dopant type and concentration [6,11,24–29].

Hydrogen bonds in stoichiometric and congruent LiNbO_3 crystals

Since different positions of hydrogen atoms bound by a hydrogen bond to an oxygen atom are found in the structure of a lithium niobate single crystal, the number and parameters of bands in the IR absorption spectrum in the region of valence vibrations of hydrogen bonds vary. Cations Li^+ and Nb^{5+} occupy their primary positions in the crystal lattice of a perfect stoichiometric LiNbO_3 crystal with $\text{Li/Nb} = 1$; point niobium defects at the lithium position Nb_{Li} and lithium vacancies V_{Li} are also lacking completely. According to the data from [3,28], the crystal lattice of such crystals features no positions for a hydrogen atom bound by a hydrogen bond to an oxygen atom. In view of this, no absorption bands related to OH^- groups should

be present in the frequency region of valence vibrations in IR absorption spectra of a perfect stoichiometric crystal.

The structure of an actual highly ordered stoichiometric single crystal (even with the Li/Nb ratio being strictly equal to unity) may feature point defects in the form of adjacent similar cations or vacancies and complex defects, which arise due to the presence of a hydrogen atom bound by a hydrogen bond to an oxygen atom in the structure of a single crystal, associated with them. Actual LiNbO_3 crystals with different Li/Nb ratios grown by HTSSG (high-temperature top-seeded solution growth) from melt of a congruent composition with K_2O flux were studied in [3,30]. The effect of the crystal composition on the frequency and shape of absorption bands in the IR spectrum in the frequency region of valence vibrations of OH^- groups was examined. According to the data obtained in [3,30], the IR spectrum of a nominally pure congruent crystal ($\text{Li/Nb} = 0.946$) featured a broad (approximately 30 cm^{-1} in width) absorption band split into several components with frequencies of 3467, 3483, and 3488 cm^{-1} . The FWHM of these absorption bands with frequencies of 3466, 3480, and 3488 cm^{-1} decreased as the composition of a LiNbO_3 crystal became closer to the stoichiometric one. A single narrow absorption band with a width of 3 cm^{-1} and a frequency of 3466 cm^{-1} was observed in the IR spectrum of an actual highly ordered stoichiometric crystal ($\text{Li/Nb} = 1$). The authors of [30] believe that the absorption band at 3466 cm^{-1} is related to the formation of a complex OH_{Li}^- defect where hydrogen occupies the primary position of Li. A similar conclusion regarding the hydrogen atom position in the LiNbO_3 crystal structure was made in [5], but the authors of this paper assumed that the lithium position occupied by a hydrogen atom is located near the long oxygen bond (336 pm). It was hypothesized in [5] that a nominally pure stoichiometric LiNbO_3 crystal may be regarded as a crystal with metallic Me^{5+} dopant. Nb^{5+} ions localized at positions extrinsic to them may be considered as this Me^{5+} dopant. Although the ratio of major components is $\text{Li/Nb} = 1$, point defects of the cation sublattice in the form of adjacent similar Nb^{5+} cations are present in the structure of a stoichiometric LiNbO_3 crystal. The authors of [5] believe that the absorption band with a frequency of 3466 cm^{-1} corresponds to the valence vibrations of an OH^- group in a complex $\text{Me}_{\text{Nb}}^{5+}-\text{OH}^-$ defect. According to the data from [12], absorption bands with frequencies of 3481 and 3489 cm^{-1} , which correspond to a complex $(V_{\text{Li}})-\text{OH}$ defect, were observed in the IR absorption spectrum of a LiNbO_3 crystal of a congruent composition in the region of valence vibrations of hydrogen bonds. The authors of this paper believe that a hydrogen atom is positioned at vacant octahedra that were previously occupied by lithium cations (V_{Li}).

Several (no more than six) broad bands, which are representative of several positions of hydrogen atoms in the crystal structure, are observed in the IR absorption spectrum in the case of any deviation from stoichiometry ($\text{Li/Nb} \neq 1$). Thus, changes in the number of hydrogen atom positions in

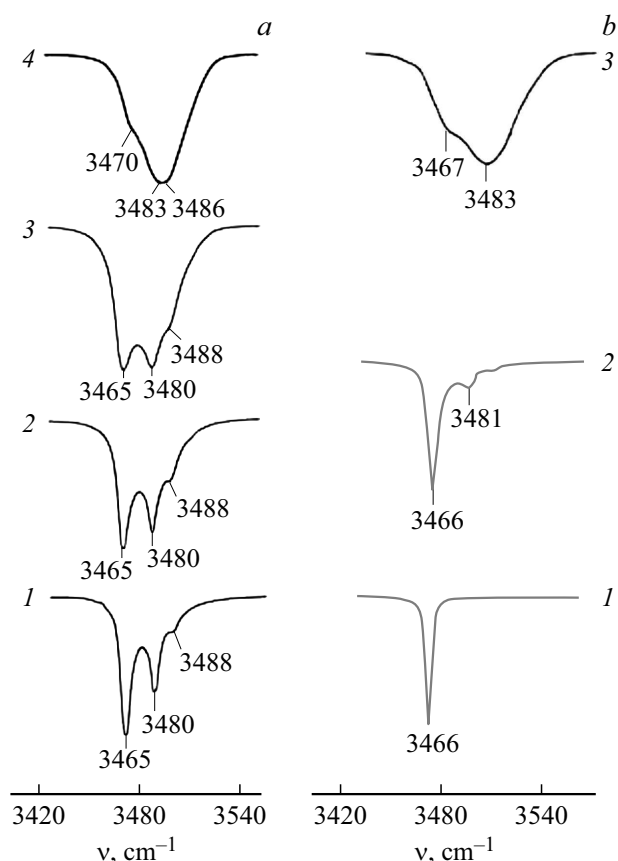


Figure 1. (a) IR absorption spectra (in relative units) in the frequency region of valence vibrations of OH^- groups of the following crystals: 1 — $\text{LiNbO}_{3\text{stoich}}$, 2 — $\text{LiNbO}_{3\text{stoich}}$ (6.0 wt.% K_2O), 3 — $\text{LiNbO}_{3\text{stoich}}$ (4.5 wt.% K_2O), and 4 — $\text{LiNbO}_{3\text{cong}}$ ($\text{Li}/\text{Nb} = 0.946$) [30,31]; (b) IR absorption spectra of crystals grown by HTTSSG with K_2O flux (1 — $\text{LiNbO}_{3\text{stoich}}$ (12.1 wt.% K_2O), 2 — $\text{LiNbO}_{3\text{stoich}}$ (9.35 wt.% K_2O) and crystal 3 — $\text{LiNbO}_{3\text{cong}}$ (48.7 mol.% Li_2O) [3].

the structure of a LiNbO_3 single crystal are reasonably indicative of the correspondence between its composition and the stoichiometric composition ($\text{Li}/\text{Nb} = 1$). The IR absorption spectra in the frequency region of valence vibrations of OH^- groups of $\text{LiNbO}_{3\text{cong}}$, $\text{LiNbO}_{3\text{stoich}}$, $\text{LiNbO}_{3\text{stoich}}:\text{K}_2\text{O}$ (4.5 wt.%), and $\text{LiNbO}_{3\text{stoich}}:\text{K}_2\text{O}$ (6.0 wt.%) crystals and the IR spectra obtained in [3] were analyzed in [31,32] (Fig. 1). Absorption bands with frequencies of 3470, 3483, and 3486 cm^{-1} were observed in [31,32] for a nominally pure congruent $\text{LiNbO}_{3\text{cong}}$ ($\text{Li}/\text{Nb} = 0.946$) crystal. Three bands of the same polarization with frequencies of 3465, 3480, and 3488 cm^{-1} were observed (Fig. 1) in the IR spectrum for $\text{LiNbO}_{3\text{stoich}}:\text{K}_2\text{O}$ crystals grown by HTTSSG in the frequency region of valence vibrations of OH^- groups. This result contradicts the data from [3,30] where only one such band was detected for crystals grown by HTTSSG. This suggests that the structure of our $\text{LiNbO}_{3\text{stoich}}:\text{K}_2\text{O}$ crystals grown by HTTSSG assumes an intermediate position between the structures of crystals of stoichiometric and

congruent compositions. As the crystal structure gets closer to the stoichiometric composition ($\text{Li}/\text{Nb} \approx 1$), the bands in IR spectra become narrower, and the intensity of bands with frequencies of 3480 and 3488 cm^{-1} decreases (Fig. 1). Thus, the data from [31,32] differ from the results presented in [3,30] where crystals were also grown by HTTSSG, but just a single absorption band with a frequency of 3466 cm^{-1} was detected (Fig. 1) in the IR absorption spectrum of an actual highly ordered stoichiometric crystal. This suggests that the positions of hydroxyl groups in an actual highly ordered stoichiometric crystal with almost zero Nb_{Li} defects are equivalent, and the system features only one value of the quasi-elastic constant of the O–H bond. Notably, this value is lower than the values of quasi-elastic constants of O–H bonds in nonstoichiometric crystals. This distinctive feature of the structure is attributable to the fact that oxygen octahedra in a highly ordered stoichiometric crystal are almost undistorted and near-perfect. All octahedra (vacant octahedron and octahedra where Nb and Li are located) in a near-perfect stoichiometric crystal are virtually equivalent (the O–O distances are almost equal), and the cation sublattice is much more ordered than the one in LiNbO_3 crystals of any other composition [2,3].

The cation sublattice of crystals grown from melt of a congruent composition is much more disordered than the cation sublattice of stoichiometric samples (primarily due to the presence of Nb_{Li} defects that act as the deepest electron traps). Owing to a change in the O–O bond length in the process of defect formation, point defects of the cation sublattice in crystals (Nb_{Li} , V_{Li} , etc.) do not only disrupt the sequence order of structural units of the cation sublattice along the polar axis, but also „perturb“ oxygen octahedra O_6 [24,31,33–35]. The degree of this „perturbation“ of octahedra (vacant ones and those occupied by Li^+ and Nb^{5+} cations) and the O–O distances in octahedra depend to a considerable extent on the Li/Nb value that basically defines the number of point defects (Nb_{Li} , V_{Li} , etc.) in undoped crystals. Owing to the presence of hydrogen in a LiNbO_3 crystal, these point defects form complexes with OH^- groups. These structural features translate into the fact that the positions of all OH^- groups and the quasi-elastic constants of the O–H bond in octahedra occupied by Li^+ and Nb^{5+} cations and in vacant octahedra are almost the same in near-perfect stoichiometric crystals. This is readily confirmed by research data [31,32]. The detection of three bands in the IR absorption spectrum of $\text{LiNbO}_{3\text{cong}}$, $\text{LiNbO}_{3\text{stoich}}$, $\text{LiNbO}_{3\text{stoich}}$ (4.5 wt.% K_2O), and $\text{LiNbO}_{3\text{stoich}}$ (6.0 wt.% K_2O) crystals is indicative of the presence of three localization centers for hydrogen atoms bound by a hydrogen bond to oxygen atoms. Point defects (V) act as such centers and form complex defects with OH^- groups. It is worth noting that the spectra of $\text{LiNbO}_{3\text{stoich}}$ and $\text{LiNbO}_{3\text{stoich}}$ (6.0 wt.% K_2O) crystals are almost identical. This suggests that these crystals have the same localization of OH^- groups and equal values of the quasi-elastic constants of O–H bonds.

Hydrogen bonds in doped LiNbO₃ crystals

The dopant type and concentration in a LiNbO₃ crystal have a significant effect on the formation and nature of complex defects, which arise due to the presence of hydrogen bonds, and on the physical properties of a crystal [3,6,7]. Specifically, point defects and complex defects associated with them, which arise due to the presence of multicharged (photorefractive) cations (Fe, Cu, etc.) cations in a crystal, have an effect on the compositional uniformity and the resistance of a crystal to optical radiation [10,12]. The presence of complex defects invariably enhances the low-temperature conductivity, suppresses photorefraction, and has a negative effect on the coercive field magnitude [3,6,12]. In order to gain an understanding of the mechanism of formation of complex defects and study the dynamics of their localization in a crystal with variation of the dopant concentration, one needs to take the valence (oxidation degree), the electronegativity, and the ionic radius of dopants into account. If several types of dopants are present in a LiNbO₃ crystal, they may compete for positions to occupy in the crystal structure.

Hydrogen bonds in single-doped LiNbO₃ crystals

Doping with „nonphotorefractive“ addition elements (Mg, Zn, Sc, In, etc.) suppresses photorefraction and reduces the coercive field magnitude in a LiNbO₃ crystal. When a LiNbO₃ crystal is doped, a change in the dopant concentration results both in a change in the Li/Nb ratio and in a redistribution of principal (lithium and niobium) and dopant cations over octahedra. An increase in the concentration of nonphotorefractive dopants in a LiNbO_{3cong} crystal occurs with two mechanisms of adjustment of the sequence order of structural units of the cation sublattice (ordering and disordering mechanisms), which compete with each other, acting alongside it. The interaction of these mechanisms is responsible in part for the emergence of concentration thresholds for dopant Zn and Mg in LiNbO₃ crystals. The properties of a crystal change dramatically (due to a change in the mechanism of inclusion of a dopant cation into the structure) when these thresholds are exceeded [2,7,10,36].

Figure 2 shows the IR absorption spectra in the frequency region of valence vibrations of OH⁻ groups of a LiNbO_{3cong} crystal and a series of LiNbO₃:Mg (0.19–5.91 mol.% MgO) and LiNbO₃:Zn (0.04–4.54 mol.% ZnO) single crystals. The concentration thresholds at 3.0 and 5.5 mol.% MgO [2] lie within the concentration range (0.19–5.91 mol.% MgO). The concentration thresholds at 5.3 and 6.8 mol.% ZnO in melt [37] also lie within the concentration range (0.04–6.5 mol.% ZnO).

The defect structure of a crystal and the formation of O–H bonds may be characterized with the use of vacancy split models and full-profile XRD analysis data [38]. According to the split model of compensation of Li vacancies, one lithium ion is substituted partially in the crystal lattice

of LiNbO_{3cong} by a niobium ion with the formation of four lithium vacancies [3,39]. A defect complex in the model of lithium vacancies consists of a point Nb_{Li} defect surrounded by three point V_{Li} defects in its immediate neighborhood and one point V_{Li}–OH defect. This defect complex has an electric dipole moment oriented along axis Z [26]. Negatively charged point (V_{Li})⁻ defects attract a hydrogen atom, which is bound by a hydrogen bond to an oxygen atom, located at long O–O bonds (336 pm). According to the data from [9], this is the mechanism of formation of complex V_{Li}–OH defects that correspond to the absorption bands with frequencies of 3483 and 3486 cm⁻¹ (Fig. 2, curve 1).

No new complex defects form at concentrations in the region of the first threshold value (~ 3.0 mol.% MgO) for LiNbO₃:Mg crystals and near the concentration threshold (~ 6.76 mol.% ZnO) in melt for LiNbO₃:Zn crystals. This is attributable to the fact that addition elements (Mg, Zn) substitute Nb_{Li} defects, thus forming (Mg_{Li}⁺, Zn_{Li}⁺) defects that are charged positively relative to the crystal lattice and cannot attract hydrogen atoms and form new complex defects. Thus, IR absorption spectra in the frequency region of valence vibrations of hydrogen bonds of LiNbO₃:Mg and LiNbO₃:Zn crystals in the region of the first „threshold“ values are similar to the IR spectrum of a nominally pure LiNbO_{3cong} crystal of a congruent composition (Fig. 2, a, curves 1–7 and Fig. 2, b, curves 1–8).

As the dopant magnesium concentration increases, Nb_{Li} defects near the second concentration threshold (~ 5.5 mol.% MgO) get displaced by Mg²⁺ cations, and Mg²⁺ cations later start occupying the positions of Li⁺ and Nb⁵⁺ cations of the perfect stoichiometric structure, thus forming point Mg_{Li}⁺ and Mg_{Nb}³⁻ defects that combine into self-compensating Mg_{Li}⁺–Mg_{Nb}³⁻ pairs being strongly attractive for a hydrogen atom. Thus, a hydrogen atom leaves a (V_{Li})–OH⁻ defect and is then involved in the formation of a complex Mg_{Li}⁺–Mg_{Nb}³⁻–OH defect that corresponds to the absorption bands with frequencies of 3526 and 3535 cm⁻¹. The emergence of these structural features also results in a shift of the absorption bands in the IR spectrum toward higher frequencies (Fig. 2, a, curve 8). However, the IR absorption spectrum after the second concentration threshold (~ 5.5 mol.% MgO) is almost identical to the spectrum of crystals with a magnesium concentration below the first threshold value (Fig. 2, a, curve 10). The authors of [26,40] associate the shift of the IR absorption bands of heavily doped LiNbO₃:Mg (> 5.5 mol.% MgO) single crystals with the formation of additional phases of magnesium niobate (Mg₄Nb₂O₉ phase). The issue of existence of an additional lithium niobate phase above the second concentration threshold is debatable, since no methods for direct determination of this low-concentration phase in a crystal are currently available. The extremely low concentration of this phase (if it does exist in a crystal) precludes one from identifying it even with the use of full-profile XRD analysis combined with calculations based on

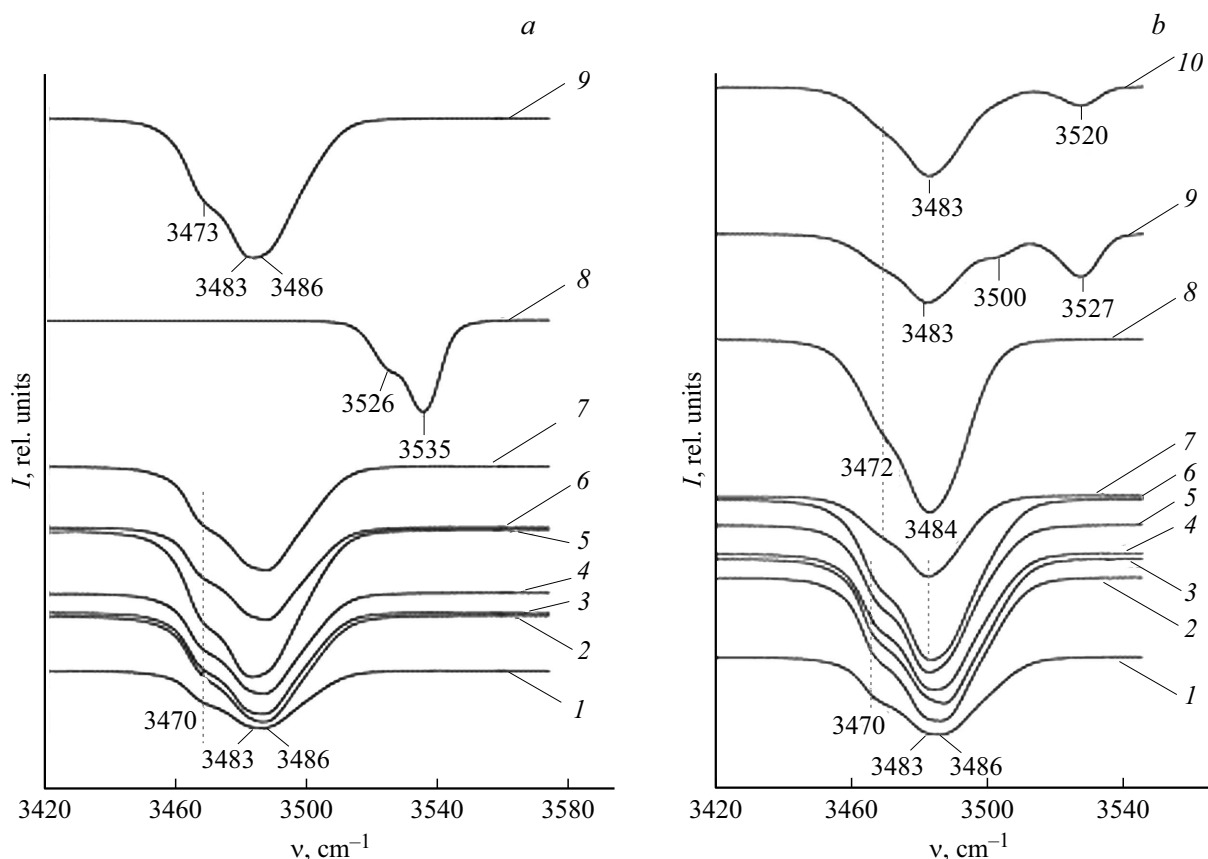


Figure 2. IR absorption spectra of single crystals in the frequency region of valence vibrations of OH^- groups (a): 1 — $\text{LiNbO}_{3\text{cong}}$ ($\text{Li}/\text{Nb}=0.946$), 2 — $\text{LiNbO}_3:\text{Mg}(0.19)$, 3 — $\text{LiNbO}_3:\text{Mg}(0.48)$, 4 — $\text{LiNbO}_3:\text{Mg}(1.53)$, 5 — $\text{LiNbO}_3:\text{Mg}(1.65)$, 6 — $\text{LiNbO}_3:\text{Mg}(2.13)$, 7 — $\text{LiNbO}_3:\text{Mg}(3.02)$, 8 — $\text{LiNbO}_3:\text{Mg}(5.29)$, 9 — $\text{LiNbO}_3:\text{Mg}(5.91 \text{ mol.}\% \text{ MgO})$; (b): 1 — $\text{LiNbO}_{3\text{cong}}$ ($\text{Li}/\text{Nb}=0.946$), 2 — $\text{LiNbO}_3:\text{Zn}(0.04)$, 3 — $\text{LiNbO}_3:\text{Zn}(0.07)$, 4 — $\text{LiNbO}_3:\text{Zn}(1.19)$, 5 — $\text{LiNbO}_3:\text{Zn}(1.40)$, 6 — $\text{LiNbO}_3:\text{Zn}(2.01)$, 7 — $\text{LiNbO}_3:\text{Zn}(4.46 \text{ mol.}\%)$, 8 — $\text{LiNbO}_3:\text{Zn}(4.54)$, 9 — $\text{LiNbO}_3:\text{Zn}(4.68)$, 10 — $\text{LiNbO}_3:\text{Zn}$ (6.5 mol.% ZnO in a crystal).

split models of the cation sublattice of a lithium niobate crystal. IR absorption spectra in the region of valence vibrations of OH groups provide indirect (although only tentative) evidence of the presence of this phase.

The cation sublattice structure also undergoes rearrangement in LiNbO_3 crystals with a zinc concentration exceeding the threshold value ($\sim 6.76 \text{ mol.}\% \text{ ZnO}$). Zinc cations start displacing niobium cations from their positions Nb_{Nb} and form point Zn_{Nb} defects. This induces significant changes in the IR absorption spectra in the region of valence vibrations of OH^- groups (Fig. 2, b, curve 9). Negatively charged point $\text{Zn}_{\text{Nb}}^{3-}$ defects have the capacity to localize hydrogen ions and form complex $\text{Zn}_{\text{Nb}}\text{-OH}$ defects. The absorption bands with frequencies ~ 3500 and 3527 cm^{-1} (Fig. 2, b, curve 9) correspond to this complex defect in the spectrum of an „above-threshold“ $\text{LiNbO}_3:\text{Zn}$ crystal (4.68 mol.% ZnO in a crystal). These absorption bands are typical of all „above-threshold“ $\text{LiNbO}_3:\text{Zn}$ crystals grown from melt with a concentration of $\text{ZnO} \geq 6.76 \text{ mol.}\%$. For example, the absorption band with a frequency of 3520 cm^{-1} in the spectrum (Fig. 2, b, curve 10) is indica-

tive of the presence of complex $\text{Zn}_{\text{Nb}}\text{-OH}$ defects in a $\text{LiNbO}_3:\text{Zn}$ crystal (6.5 mol.% ZnO in a crystal).

Hydrogen bonds in double-doped LiNbO_3 crystals

According to the data from [3,37], double doping of LiNbO_3 crystals with „nonphotorefractive“ and „photorefractive“ cations provides an opportunity for finer adjustment of ordering of structural units of the cation sublattice and distortion of oxygen octahedra O_6 , which define the magnitude of spontaneous polarization and the ferroelectric properties of a crystal, by dopants and allows one to alter the type and number of defects with localized electrons, which define the magnitude of photorefraction [3]. Thus, a double-doped LiNbO_3 single crystal may be more compositionally uniform than a single-doped one [37]. Photovoltaic active dopants in the form of multicharged cations of transition metals (e.g., Fe) affect the compositional uniformity and the optical resistance of a crystal [3,41–43]. If one dopant is „photorefractive“, double doping allows one to engineer optical materials with a minimum photorefractive response time and an increased resistance to optical damage [44].

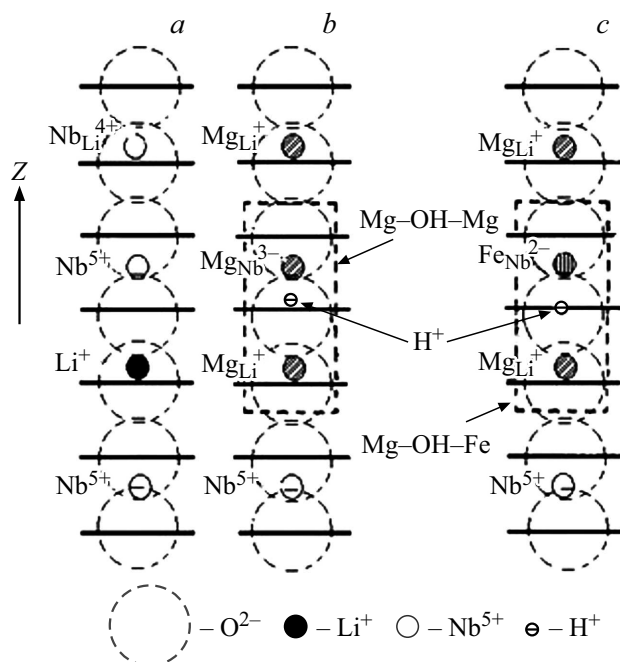


Figure 3. Defects structure of crystals: $\text{LiNbO}_{3\text{cong}}$ ($\text{Li/Nb}=0.946$) (a) and $\text{LiNbO}_3:\text{Mg}$ (5.05 mol.% MgO): Fe (0.009 mol.% Fe_2O_3) (b, c).

Owing to its small size and a relatively high diffusion rate, a hydrogen atom in a LiNbO_3 crystal is located close to negatively charged point defect centers. Figure 3 presents the model of arrangement of complex defects in the structure of a congruent $\text{LiNbO}_3:\text{Mg}:\text{Fe}$ crystal. The model in Fig. 3 is based on the common patterns of inclusion of dopants into the structure of a congruent LiNbO_3 crystal studied in [2,10] and the arguments regarding the presence and positioning of a hydrogen atom in a LiNbO_3 crystal [4]. Almost all structural Nb_{Li} defects in a $\text{LiNbO}_3:\text{Mg}:\text{Fe}$ crystal doped with magnesium above the second concentration threshold (5.5 mol.% MgO in melt) are displaced by Mg^{2+} cations; as the concentration increases further, Mg^{2+} cations start occupying the primary positions of Li^+ and Nb^{5+} cations of the perfect stoichiometric structure and forming Mg_{Li} and Mg_{Nb} defects. The emergence of defect Fe_{Nb} centers at the primary positions of Nb_{Nb} displaced by Fe^{3+} cations occurs alongside with the formation of Mg_{Li} and Mg_{Nb} defects. The following self-compensating pairs form: $\text{Mg}_{\text{Li}}^+ - \text{Mg}_{\text{Nb}}^{3-}$ and $\text{Mg}_{\text{Li}}^+ - \text{Fe}_{\text{Nb}}^{2-}$. These pairs feature a high effective negative charge and are thus strongly attractive for a hydrogen atom bound by a hydrogen bond to an oxygen atom. All this results in the formation of a complex $\text{Mg}_{\text{Li}} - \text{OH} - \text{M}_{\text{Nb}}$ defect, which corresponds to the IR absorption bands with frequencies of 3526 and 3535 cm^{-1} (Fig. 4, curve 4), and a complex $\text{Mg}_{\text{Li}} - \text{OH} - \text{Fe}_{\text{Nb}}$ defect, which corresponds to the absorption band with a frequency of 3506 cm^{-1} .

According to the data presented in [25], iron cations $\text{LiNbO}_3:\text{Mg}(5.05):$

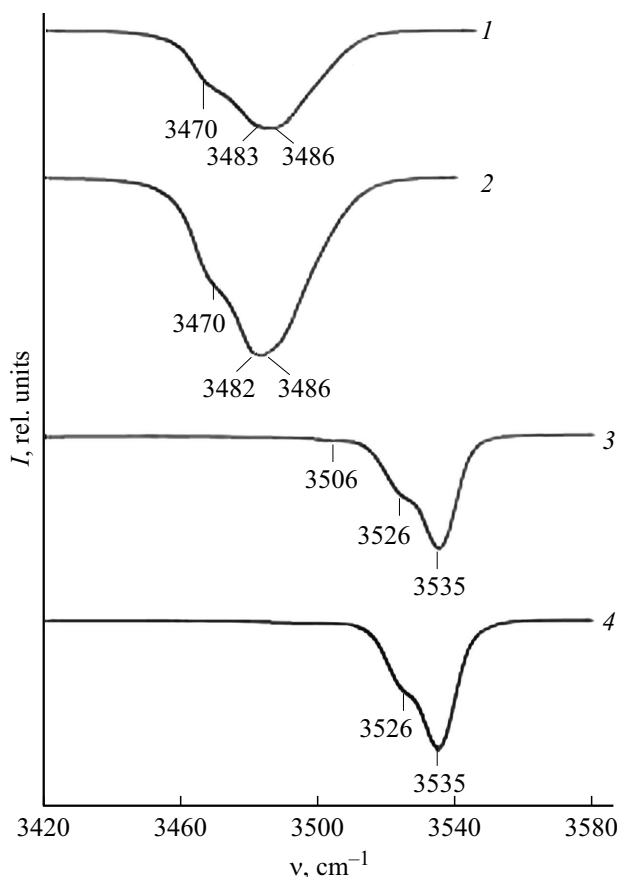


Figure 4. IR absorption spectra of lithium niobate single crystals in the frequency region of valence vibrations of OH^- groups: 1 — $\text{LiNbO}_{3\text{cong}}$ ($\text{Li/Nb}=0.946$), 2 — $\text{LiNbO}_3:\text{Y}$ (0.24): Mg : (0.63 wt.%), 3 — $\text{LiNbO}_3:\text{Gd}$ (0.25): Mg (0.75 wt.%), 4 — $\text{LiNbO}_3:\text{Mg}$ (5.05): Fe (0.009 mol.%). $T = 293$ K [12].

: Fe (0.009 mol.%) reduce the concentration of OH^- groups. Fe cations in a grown crystal exist in complex with OH^- groups. The number of OH ions spent on the formation of these complex defects increases with the concentration of Fe cations in melt. In other words, the higher the concentration of iron in a $\text{LiNbO}_3:\text{Mg}:\text{Fe}$ crystal, the lower then concentration of other defect complexes with OH^- groups in this crystal.

The positioning of hydrogen atoms at long O—O bonds (336 pm) corresponds to considerably higher frequencies of valence vibrations of OH^- groups than the positioning of hydrogen at shorter bonds [6,45]. In our view, the difference in electronegativities (Mg^{2+} (~ 1.3) and Fe^{3+} (~ 1.8)) and ionic radii of principal and dopant cations may also contribute to the difference in frequencies (and, consequently, the quasi-elastic constants of O—H bonds) in the spectra of a congruent crystal and a $\text{LiNbO}_3:\text{Mg}(5.05 \text{ mol.}\% \text{ MgO}):\text{Fe}(0.009 \text{ mol.}\% \text{ Fe}_2\text{O}_3)$ crystal. According to the data from [46], the absorption bands in the IR spectrum are close in frequency and overlap considerably if the dopant cation radius is close to the radius of principal cations Li^+ and Nb^{5+} . If this is not the

case, the absorption bands are separate. The ionic radius of multicharged cations Fe^{3+} (0.67 Å) is larger than the radii of Mg^{2+} (0.65 Å), Li^+ (0.66 Å), and Nb^{5+} (0.66 Å) ions [47]. All this contributes to a shift of the frequencies of valence vibrations of OH^- groups in the spectrum of a $\text{LiNbO}_3:\text{Mg}(5.05):\text{Fe}(0.009 \text{ mol.}\%)$ crystal (Fig. 4) toward higher frequencies. The shift indicates that the quasi-elastic constants of O–H bonds and the „perturbation“ of oxygen octahedra O_6 in doped crystals are greater than those in a congruent LiNbO_3 crystal.

The specific feature of positioning of trivalent rare-earth (RE) dopants in the structure of a LiNbO_3 crystal is the availability of four cation positions: three octahedral positions (Li^+ , Nb^{5+} , vacant octahedron) and an intermediate tetrahedral position. Codoping with a trivalent RE dopant results in the emergence of four types of self-compensating pairs [48]. However, one needs to take the valence, the relative electronegativity, and the ionic radius of dopants into account in order to gain a complete understanding of the mechanism of inclusion of dopants. The ionic radius of RE metal dopants is larger than the ionic radii of Li^+ (0.66 Å) and Mg^{2+} (0.65 Å) cations. The relative electronegativity of RE metals varies from 1.1 to 1.3. It is much closer to the relative electronegativity of magnesium Mg^{2+} (1.31) cations than to the electronegativity of Li^+ (0.98). Thus, the existence of self-compensating $\text{Mg}_{\text{Li}}-\text{RE}_{\text{Nb}}$ and $\text{Mg}_{\text{Li}}-\text{Mg}_{\text{Nb}}$ pairs appears feasible. It was demonstrated in [48,49] that trivalent RE ions in a LiNbO_3 crystal mostly occupy the positions of Li^+ . A slight distortion of the crystal lattice due to the large radius of a RE ion induces a shift of RE ions from the Li position: they are shifted by 0.46 Å along ferroelectric axis Z [48–50]. It was assumed in experimental and theoretical studies [51,52] that RE ions in the structure of a LiNbO_3 crystal occupy the primary Nb^{5+} positions. This agrees with the data on the positioning of RE ions in $\text{LiNbO}_3:\text{Mg}:\text{RE}$ crystals presented in [53,54]. It was hypothesized in [33,45] that the additional absorption bands in IR spectra in the region of valence vibrations of hydrogen bonds in congruent $\text{LiNbO}_3:\text{Mg}:\text{RE}$ and $\text{LiNbO}_3:\text{RE}$ crystals are associated with the formation of new complex defects. These defect complexes form in such crystals when a certain threshold RE dopant concentration is exceeded. The threshold concentration for RE dopants implies that RE ions are located at the Nb position of the LiNbO_3 crystal lattice.

According to the data from [4], a considerable fraction of trivalent ions in $\text{LiNbO}_3:\text{Y}:\text{Mg}$ crystals occupies random positions in the LiNbO_3 crystal lattice and does not substitute (even partially) point Nb_{Li} and V_{Li} defects and niobium cations located at the primary positions of the perfect crystal structure. Since the concentration of magnesium in this crystal reaches the second threshold value ($\sim 5.5 \text{ mol.}\%$ MgO in melt), a complex $\text{Mg}_{\text{Li}}^+-\text{Mg}_{\text{Nb}}^{3-}-\text{OH}^-$ defect, which corresponds to the absorption band with a frequency of 3535 cm^{-1} (Fig. 4, curve 4), forms in the structure of a $\text{LiNbO}_3:\text{Y}:\text{Mg}$ crystal. Dopant trivalent Y^{3+} cations in a complex $\text{Mg}-\text{OH}-\text{Y}^{3+}$ defect may substitute either Li

or Nb positions [55]. Absorption bands corresponding to new complex defects induced by the presence of OH^- groups in a crystal are then lacking in the IR spectrum. Excess niobium cations in a $\text{LiNbO}_{3\text{cong}}$ crystal behave in a similar way. This provides an explanation for the similarity between the IR absorption spectra of a $\text{LiNbO}_{3\text{cong}}$ crystal and a double-doped $\text{LiNbO}_3:\text{Y}(0.24):\text{Mg}:(0.63 \text{ wt.}\%)$ crystal (Fig. 4, curves 1 and 2).

The IR spectrum of a $\text{LiNbO}_3:\text{Gd}(0.25):\text{Mg}(0.75 \text{ wt.}\%)$ crystal is shifted by $\sim 50 \text{ cm}^{-1}$ toward higher frequencies (Fig. 4, curve 3) due to the fact that the ionic radius (111 pm) and the atomic weight (157) of dopant Gd exceed the corresponding parameters of Nb (66 pm and 92), Li (66 pm and 7), and Y (106 pm and 89). The inclusion of dopant Gd^{3+} cations into the crystal lattice structure alters the oxygen octahedron and extends the oxygen bond. This, in turn, results in an increase in the frequency of valence vibrations of OH groups and explains the shift of the $\text{LiNbO}_3:\text{Gd}(0.25):\text{Mg}(0.75 \text{ wt.}\%)$ crystal spectrum toward longer wavelengths.

Conclusion

Thus, hydrogen atoms present in the structure of a LiNbO_3 crystal form complex defects with principal (Nb^{5+} and Li^+) and dopant (Me) cations and vacancies (V): $\text{V}_{\text{Li}}-\text{OH}$, $\text{Nb}_{\text{Li}}-\text{OH}$, $\text{Me}-\text{OH}$, $\text{Me}-\text{OH}-\text{Me}$, etc. Since different positions of hydrogen atoms bound by hydrogen bonds to an oxygen atom are found in the structure of a lithium niobate single crystal, the number and parameters of absorption bands in the IR spectrum in the region of valence vibrations of hydrogen bonds vary. A single narrow absorption band with a width of 3 cm^{-1} and a frequency of 3466 cm^{-1} was observed in the IR spectrum of an actual highly ordered stoichiometric crystal ($\text{Li}/\text{Nb} = 1$) with a high degree of structural perfection. This is indicative of the fact that hydrogen atoms have one position in the structure of a LiNbO_3 crystal. Several (no more than six) broad absorption bands, which are representative of several positions of hydrogen atoms in the crystal structure, are observed in the spectrum in the case of any deviation from stoichiometry ($\text{Li}/\text{Nb} \neq 1$). Thus, changes in the number of hydrogen atom positions in the structure of a LiNbO_3 single crystal are reasonably indicative of the correspondence between its composition and the stoichiometric composition ($\text{Li}/\text{Nb} = 1$). This fact allowed us to determine that near-stoichiometric ($\text{Li}/\text{Nb} \sim 1$) $\text{LiNbO}_{3\text{stoich}}$ (6.0 wt.% K_2O) crystals grown by HTSSG at Kristall-2 growth units from congruent melt with the addition of $\sim 6.0 \text{ wt.}\%$ K_2O flux may have approximately the same defect structure of the hydrogen atom sublattice as the one in stoichiometric $\text{LiNbO}_{3\text{stoich}}$ crystals grown from melt containing $\sim 58.6 \text{ mol.}\%$ Li_2O and be considerably superior to $\text{LiNbO}_{3\text{stoich}}$ crystals in terms of their overall optical and structural uniformity [31,32].

Changes in the IR absorption spectrum in the frequency region of valence vibrations of OH⁻ groups of LiNbO₃:Me (Me = Zn, Mg, Y, Gd) crystals are induced by the formation of complex defects of different types: Me_{Li}-OH⁻, Me_{Li}-Me_{Nb}-OH. Point Me_{Li} and Me_{Nb} defects at Li and Nb cation positions of the perfect stoichiometric structure form a self-compensating Me_{Li}-Me_{Nb} pair that is strongly attractive for hydrogen atoms bound by a hydrogen bond to oxygen atoms. This leads to the formation of a complex Me_{Li}-Me_{Nb}-OH defect. The obtained data suggest that the nature of complexation of OH groups with point defects of the cation sublattice changes on passing through the concentration thresholds. The IR absorption spectra in the frequency region of valence vibrations of hydrogen bonds of a series of LiNbO₃:Mg and LiNbO₃:Zn crystals with the dopant concentration below the first concentration threshold are similar to the IR spectrum of a nominally pure crystal of a congruent composition. As the dopant concentration approaches the second concentration threshold (~ 5.5 mol.% MgO and ~ 7 mol.% ZnO), Nb_{Li} defects are displaced gradually by Mg and Zn cations. Mg and Zn cations then start occupying the positions of Li and Nb cations of the perfect stoichiometric structure and forming complex Mg(Zn)_{Li}-OH and Mg(Zn)_{Nb}-OH defects that correspond to the absorption bands with frequencies of 3526 and 3535 cm⁻¹.

Our analysis of mechanisms of formation of complex defects in a double-doped LiNbO₃:Mg(5.05):Fe (0.009 mol.%) crystal revealed the emergence of complex (Fe_{Nb})-OH-(Mg_{Li}), (Mg_{Li})-(Mg_{Nb})-OH defects. The coefficient of inclusion of Fe cations decreases due to the presence of Mg cations in a crystal. At the same time, even an insignificant concentration of Fe cations in a crystal alters the parameters of the unit cell of a LiNbO₃:Mg:Fe crystal and the polarizability of oxygen octahedra, thus leading to a change in the optical properties of this crystal.

Conflict of interest

The authors declare that they have no conflict of interest.

References

- [1] Yu.S. Kuz'minov, *Elektroopticheskie i nelineinoopticheskie kristall niobata litiya* (Nauka, M., 1987) (in Russian).
- [2] N.V. Sidorov, T.R. Volk, B.N. Mavrin, V.T. Kalinnikov, *Niobat litiya: defekty, fotorefraktsiya, kolebatel'nyi spektr, polarizatsiya* (Nauka, M., 2003) (in Russian).
- [3] K. Lengyel, A. Peter, L. Kovacs, G. Corradi, L. Palfavi, J. Hebling, M. Unferdorben, G. Dravecz, I. Hajdara, Zs. Szaller, K. Polgar. *Appl. Phys. Rev.*, **2**, 040601 (2015). DOI: 10.1063/1.4929917
- [4] L. Kovacs, M. Wöhlecke, A. Jovanovic, K. Polgar, S. Kapphan. *J. Phys. Chem. Sol.*, **52** (6), 797 (1991). DOI: 10.1016/0022-3697(91)90078-E
- [5] L. Kovacs, Zs. Szaller, K. Lengyel, G. Corradi. *Opt. Mat.*, **37**, 55 (2014). DOI: 10.1016/j.optmat.2014.04.043
- [6] J.M. Cabrera, J. Olivares, M. Carrascosa, J. Rams, R. Müller, E. Diéguez. *Adv. Phys.*, **45** (5), 349 (1996). DOI: 10.1080/00018739600101517
- [7] L. Arizmendi, E.J. Ambite, J.L. Plaza. *Opt. Mat.*, **35** (12), 2411 (2013). DOI: 10.1016/j.optmat.2013.06.043
- [8] Z. Galazka. *J. Cryst. Growth.*, **178** (3), 345 (1997). DOI: 10.1016/S0022-0248(96)01159-1
- [9] K. Lengyel, L. Kovacs, A. Peter, K. Polgar, G. Corradi, A. Baraldi, R. Capelletti. *Appl. Phys. Lett.*, **96**, 191907 (2010). DOI: 10.1063/1.3428772
- [10] T. Volk, M. Wöhlecke. *Lithium niobate. Defects, photorefractive and ferroelectric switching* (Springer, Berlin, 2008).
- [11] Y. Kong, W. Zhang, X. Chen, J. Xu, G. Zhang. *J. Phys. Cond. Mat.*, **11** (9), 2139 (1999). DOI: 10.1088/0953-8984/11/9/010
- [12] Y. Kong, J. Xu, W. Zhang, G. Zhang. *J. Phys. Chem. Sol.*, **61** (8), 1331 (2000). DOI: 10.1016/S0022-3697(99)00413-8
- [13] S.V. Yevdokimov, A.V. Yatsenko. *Cryst. Rep.*, **48** (4), 542 (2003). DOI: 10.1134/1.1595175
- [14] A.N. Lazarev, Ya.I. Ryskin, G.P. Stavitskaya, *Kolebaniya oksinykh reshetok* (Nauka, L., 1980) (in Russian).
- [15] M. Engelsberg, R.E. de Souza, L.H. Pacobahyba, G.C. do Nascimento. *Appl. Phys. Lett.*, **67**, 359 (1995). DOI: 10.1063/1.114628
- [16] A.V. Yatsenko, *Ukr. Fiz. Zh.*, **44** (3), 411 (1999).
- [17] S.C. Abrahams, P. March. *Acta Crystallogr., Sect. B: Struct. Sci.*, **42** (2), 61 (1986). DOI: 10.1107/S0108768186098567
- [18] S.C. Abrahams. *Properties of Lithium Niobate* (Pergamon, New York, 1989).
- [19] S.C. Abrahams, J.M. Reddy, J.L. Bernstein. *J. Phys. Chem. Sol.*, **27** (6/7), 997 (1966). DOI: 10.1016/0022-3697(66)90072-2
- [20] Y. Watanabe, T. Sota, K. Suzuki, N. Iyi, S. Kimura. *J. Physics: Condens. Matter.*, **7** (18), 3627 (1995). DOI: 10.1088/0953-8984/7/18/025
- [21] Y. Furukawa, K. Kitamura, S. Tadekawa, K. Niwa, Y. Yajima, N. Iyi, I. Mnushkina, P. Guggenheim, J.M. Martin. *J. Cryst. Growth.*, **211** (1-4), 230 (2000). DOI: 10.1016/S0022-0248(99)00794-0
- [22] K. Lengyel, V. Timon, A. Hernandez-Laguna, V. Szalay, L. Kovacs. *IOP Conf. Ser.: Mater. Sci. Eng.*, **15**, 012015 (2010). DOI: 10.1088/1757-899X/15/1/012015
- [23] H.H. Nahm, C.H. Park. *Appl. Phys. Lett.*, **78** (24), 3812 (2001). DOI: 10.1063/1.1376667
- [24] J.R. Herrington, B. Dischler, A. Räuber, J. Schneider. *Sol. Stat. Commun.*, **12** (5), 351 (1973). DOI: 10.1016/0038-1098(73)90771-0
- [25] M. Cochez, M. Ferriol, P. Bourson, M. Aillerie. *Opt. Mater.*, **21** (4), 775 (2003). DOI: 10.1016/S0925-3467(02)00098-8
- [26] K. Lengyel, L. Kovacs, A. Peter, K. Polgar, G. Corradi. *Appl. Phys. B: Lasers and Optics.*, **87** (2), 317 (2007). DOI: 10.1007/s00340-007-2589-7
- [27] L. Kovacs, I. Foldvari, I. Cravero, K. Polgar, R. Capelletti. *Phys. Lett. A.*, **133** (7-8), 433 (1988). DOI: 10.1016/0375-9601(88)90931-0
- [28] A. Gröne, S. Kapphan. *J. Phys. Chem. Sol.*, **56** (5), 687 (1995). DOI: 10.1016/0022-3697(94)00184-7
- [29] R. Bhatt, S. Kar, K.S. Bartwal, V. Shula, P. Sen, P.K. Sen, V.K. Wadhawan. *Ferroelectrics*, **323** (1), 165 (2005). DOI: 10.1080/00150190500309148
- [30] K. Polgar, A. Peter, L. Kovacs, G. Corradi, Zs. Szaller. *J. Cryst. Growth.*, **177** (3-4), 211 (1997). DOI: 10.1016/S0022-0248(96)01098-6

- [31] N.V. Sidorov, M.N. Palatnikov, L.A. Bobreva, S.A. Klimin. *Inorg. Mater.*, **55** (4), 365 (2019). DOI: 10.1134/S0020168519040137
- [32] N.V. Sidorov, M.N. Palatnikov, L.A. Bobreva. *J. Structural Chemistry*, **60**, 1434 (2019). DOI: 10.26902/JSC_id46180
- [33] X.Q. Feng, J.F. Ying, Y.A. Wu, J.C. Liu. *Chin. Sci. Bull.*, **36**, 297 (1991).
- [34] A. Reisman, F. Holtzberg. *J. Amer. Chem. Soc.*, **80**, 6503 (1958). DOI: 10.1021/ja01557a010
- [35] N.V. Sidorov, P.G. Chufyrev, M.N. Palatnikov, V.T. Kalinnikov, *Nano- Mikrosist. Tekh.*, (3), 12 (2006) (in Russian).
- [36] J.J. Liu, W.L. Zhang, G.Y. Zhang. *Phys. St. Sol. A.*, **156** (2), 285 (1996). DOI: 10.1002/pssa.2211560207
- [37] M.N. Palatnikov, N.V. Sidorov, O.V. Makarova, I.V. Biryukova, *Fundamental'nye aspekty tekhnologii sil'no legirovannykh kristallov niobata litiya* (Izd. Kol'sk. Nauchn. Tsentra Ross Akad. Nauk, Apatity, 2017) (in Russian).
- [38] M.N. Palatnikov, N.V. Sidorov, D.V. Manukovskaya, O.V. Makarova, L.A. Aleshina, A.V. Kadetova. *J. American Ceramic Society*, **100** (8), 3703 (2017). DOI: 10.1111/jace.14851
- [39] N. Iyi, K. Kitamura, F. Izumi, J.K. Yamamoto, T. Hayashi, H. Asano, S. Kimura. *J. Sol. State Chem.*, **101**, 340 (1992). DOI: 10.1016/0022-4596(92)90189-3
- [40] B.C. Grabmaier, F. Otto. *J. Cryst. Growth.*, **79** (1-3), 682 (1986). DOI: 10.1016/0022-0248(86)90537-3
- [41] T. Zhang, B. Wang, F.R. Ling, S.-Q. Fang, Y.-H. Xu. *Mater. Chem. Phys.*, **83** (2-3), 350 (2004). DOI: 10.1016/j.matchemphys.2003.10.010
- [42] H. Wang, J. Wen, B. Li, H. Wang. *Phys. St. Sol. (a)*, **118** (1), K47 (1990). DOI: 10.1002/pssa.2211180151
- [43] X.H. Zhen, L.C. Zhao, Y.H. Xu. *Appl. Phys. B.*, **76** (6), 655 (2003). DOI: 10.1007/s00340-003-1158-y
- [44] Y. Fan, C. Xu, S. Xia, C. Guan, L. Cao, Q. He, G. Jin. *J. Cryst. Growth.*, **312**, 1875 (2010). DOI: 10.1016/j.jcrysgro.2010.03.001
- [45] L. Kovács, L. Rebouta, J.C. Soares, M.F. da Silva, M. Hage-Ali, J.P. Stoquert, P. Siffert, J.A. Sanz-Garcia, G. Corradi, Z. Szaller, K. Polgar. *J. Phys-Condens. Matt.*, **5**, 781 (1993).
- [46] Y. Kong, J. Deng, W. Zhang, J. Wen, G. Zhang, H. Wang. *Phys. Lett. A.*, **196** (1-2), 128 (1994). DOI: 10.1016/0375-9601(94)91057-X
- [47] I.T. Goronovskii, Yu.P. Nazarenko, E.F. Nekryach, *Kratkii spravochnik po khimii*, 5th ed., Ed. A.T. Pilipenko (Nauk. Dumka, Kyiv, 1987) (in Russian).
- [48] L. Rebouta, P.J.M. Smulders, D.O. Boerma, F. Aguillo, Lopez, M.F. da Silva, J.C. Soares. *Phys. Rev. B.*, **48**, 3600 (1993). DOI: 10.1103/PhysRevB.48.3600
- [49] A. Lorenzo, H. Jaffrezic, B. Roux, G. Boulon, J. Garcia-Sole. *Appl. Phys. Lett.*, **67** (25), 3735 (1995). DOI: 10.1063/1.115366
- [50] T. Gog, M. Griebenow, G. Materlik. *Phys. Lett. A.*, **181** (5), 417 (1993). DOI: 10.1016/0375-9601(93)90398-J
- [51] G. Burns, D.F. O'kane, R.S. Title. *Phys. Rev.*, **167** (2), 314 (1968). DOI: 10.1103/PhysRev.167.314
- [52] T. Tsuboi, S.M. Kaczmarek, G. Boulon. *J. Alloys Compd.*, **380** (1-2), 196 (2004). DOI: 10.1016/j.jallcom.2004.03.043
- [53] H.-N. Dong, S.-Y. Wu, W.-C. Zheng. *J. Phys. Chem. Sol.*, **64** (4), 695 (2003). DOI: 10.1016/S0022-3697(02)00381-5
- [54] S.H. Choh, J.H. Kim, I.-W. Park, H.J. Kim, D. Choi, S.S. Kim. *Appl. Magn. Reson.*, **24**, 313 (2003). DOI: 10.1007/BF03166932
- [55] L. Kovacs, L. Kocsor, Z. Szaller, I. Hajdara, G. Dravec, K. Lengyel, G. Corradi. *Crystals*, **7** (8), 230 (2017). DOI: 0.3390/cryst7080230